



Cite this: *Green Chem.*, 2021, **23**, 1758

Metal-free photocatalytic aerobic oxidation of biomass-based furfural derivatives to prepare γ -butyrolactone†

Rui Zhu,[‡] Gongyu Zhou,[‡] Jia-nan Teng, Wanying Liang, Xinglong Li and Yao Fu *

Efficient catalytic oxidative C–C bond cleavage with dioxygen is useful and challenging to prepare oxygenated fine chemicals from biomass. Herein, we report a catalytic strategy for the preparation of γ -butyrolactone (GBL) by photocatalytic oxidation of tetrahydrofurfuryl alcohol (THFA), tetrahydrofurfuric acid (THFCA), or other furfural derivatives at room temperature under visible-light irradiation. Metal-free mesoporous graphitic carbon nitride was used as the photocatalyst and O₂ was used as the oxidant. The effects of various semiconductor catalysts, light sources with different wavelengths, and the reaction time on the photocatalytic oxidation of THFA to GBL were separately investigated. Furthermore, the reaction mechanism was investigated through serious control experiments and the reaction pathway was investigated through density functional theory (DFT) calculations.

Received 15th December 2020,
Accepted 14th January 2021

DOI: 10.1039/d0gc04234j

rsc.li/greenchem

Introduction

Extensive utilization of fossil resources and the associated environment pollution are well-recognized problems of paramount importance in modern society.¹ Developing environmentally friendly, renewable alternative resources is of great importance for the renewable production of fine chemicals. Lignocellulose (cellulose, hemicellulose and lignin),² as an important biomass resource, has been developed rapidly in recent years. Many platform compounds,³ such as levulinic acid (LA),⁴ 5-hydroxymethyl furfural (5-HMF),⁵ and furfural,⁶ can be obtained by the catalytic conversion of lignocellulose. The preparation of high value-added chemicals through the catalytic conversion of these platform molecules obtained from renewable resources is still the current research focus.⁷ Some breakthroughs have also been achieved through the efforts of many scientists. Nevertheless, we still need to develop much more renewable resource-based reaction strategies. This is still of great significance for energy, environment, chemicals and other fields.

γ -Butyrolactone (GBL),⁸ a five-membered ring lactone, is widely used in the fields of material synthesis, pharmaceutical

intermediates, perfumes, chemical synthesis and so on. In particular, GBL is considered as a desirable bio-derived monomer for the biopolyester poly(γ -butyrolactone) in the field of polyester materials.⁹ Generally, GBL is considered as a key downstream chemical of succinic acid.¹⁰ However, harsh reaction conditions (such as high temperature and high pressure) are the shortcomings of this reaction. Therefore, great efforts still need to be made to develop various catalytic strategies for preparing GBL. The oxidative lactonization of diols, involving sequential oxidation of an alcohol and an intermediate hemiacetal (lactol), is an appealing route to these molecules.^{11–15} Numerous stoichiometric oxidants and catalytic methods have been explored to achieve this goal.¹¹ Aerobic oxidation methods offer a compelling alternative. However, the existing catalysts also face the limitations associated with harsh reaction conditions, restricted functional group tolerance, and poor chemoselectivity.¹² In addition to the above methods, GBL can also be prepared by hydrogenation reduction of succinic anhydride,¹⁶ lactonization of hydroxybutyric acid,¹⁷ Baeyer–Villiger oxidation of cyclobutanone¹⁸ and catalytic oxidative C–C bond cleavage of cyclohexanol.¹⁹ Although there have been many synthesis methods for preparing GBL, it is still of great significance to develop more synthetic methods to achieve the efficient and green preparation of GBL.

Recently, organic semiconductor materials have attracted widespread attention owing to their excellent chemical stability and green and efficient photocatalytic properties.²⁰ In addition, they also have a suitable band gap between the valence and conduction bands,²¹ which provides the possibility for oxidation or reduction of many substrates. Recently,

Hefei National Laboratory for Physical Sciences at the Microscale, iChEM CAS Key Laboratory of Urban Pollutant Conversion, Anhui Province Key Laboratory of Biomass Clean Energy, University of Science and Technology of China, Hefei, Anhui, 230026, P. R. China. E-mail: fuyao@ustc.edu.cn

†Electronic supplementary information (ESI) available. See DOI: 10.1039/d0gc04234j

‡These authors contributed equally to this work.

scientists have developed various catalytic systems based on organic semiconductor materials driven by the demand for green and sustainable chemistry. Among various organic semiconductor materials, mesoporous graphitic carbon nitride is widely used in water splitting,²² selective oxidation²³ and photoredox catalytic organic transformations²⁴ of organic molecules because of its facile synthesis and excellent photocatalytic reactivity. The properties of large surface area, plenty of vacancies and high photocatalytic activity all make mesoporous graphitic carbon nitride a promising catalyst for many reactions.

In this manuscript, we reported a catalytic strategy for the preparation of γ -butyrolactone (GBL) by photocatalytic oxidation of tetrahydrofurfuryl alcohol (THFA),²⁵ tetrahydrofurfuric acid (THFCA),²⁶ or other furfural derivatives²⁷ at room temperature under visible-light irradiation (as shown in Scheme 1). Metal-free M-CNU (mesoporous graphitic carbon nitride, prepared from urea) was used as the photocatalyst and O₂ (O₂ balloon or air) was used as the oxidant. We separately investigated the effects of various semiconductor catalysts, light sources with different wavelengths, and the reaction time on the photocatalytic oxidation of THFA to GBL. Furthermore, we also investigated the reaction mechanism through serious control experiments and the reaction pathway was further investigated through density functional theory (DFT) calculations.

Experimental

Preparation of graphitic carbon nitride

Graphitic carbon nitride was synthesized according to a previous work.²⁸ Briefly, about 40 g urea or melamine was directly heated at 550 °C for 4 h (heating rate: 2.5 °C min⁻¹) under a nitrogen atmosphere, giving a pale-yellow solid denoted as CNU or CNM respectively.

Mesoporous graphitic carbon nitride was synthesized according to a previous work.²⁹ Briefly, about 40 g urea was dissolved in a solution of 0.2 M HCl (60 mL) and ethanol (52 mL) under vigorous stirring, and tetraethyl orthosilicate (32 mL) was then slowly added to the above solution drop by drop. After stirring vigorously at room temperature for 3 h, the mixture was heated under vacuum for solvent evaporation and then dried at 100 °C for about 12 h. The obtained white solid was heated at 550 °C for 4 h (heating rate: 2.5 °C min⁻¹) under

a nitrogen atmosphere. Subsequently, hydrofluoric acid was used to remove SiO₂. Then, the obtained pale-yellow solid was washed with water and ethanol several times and dried at 80 °C for about 12 h. A pale-yellow solid (about 4 g) was finally obtained and denoted as M-CNU.

Other semiconductor materials (such as TiO₂, WO₃, MoS₂, CdS, and Al₂O₃) were purchased and used directly without any further treatment in this work.

Preparation of 2,5-dihydroxymethyltetrahydrofuran and tetrahydrofurandicarboxylic acid

2,5-Dihydroxymethyltetrahydrofuran was prepared from 5-hydroxymethylfurfural (5-HMF) by hydrogenation experiments.³⁰ A 25 mL stainless steel autoclave with a stir bar was charged with 1.8 g of 5-HMF, RANEY® nickel catalyst (100 mg) and 10 mL of ethanol. The stainless steel autoclave was purged 3 times with nitrogen and 2 times with hydrogen. Then the autoclave was pressurized to 5 MPa with hydrogen and heated to 120 °C for 3 hours. After cooling, the stainless steel autoclave was vented and the solids were separated by filtration. The acetic acid solution was evaporated under vacuum to provide about 1.5 g of 2,5-dihydroxymethyltetrahydrofuran.

Tetrahydrofuran-2,5-dicarboxylic acid was prepared from furan-2,5-dicarboxylic acid (FDCA) by hydrogenation experiments. A 25 mL autoclave with a stir bar was charged with 2.0 g of furan-2,5-dicarboxylic acid (FDCA), 0.1 g of 10% Pd/C and 10 mL of acetic acid. The autoclave was purged 3 times with nitrogen and 2 times with hydrogen. Then the autoclave was pressurized to 4 MPa with hydrogen and heated to 150 °C for 3 hours. After cooling, the autoclave was vented and the solids were separated by filtration. The acetic acid solution was evaporated under vacuum to provide about 1.6 g of tetrahydrofuran-2,5-dicarboxylic acid.

General procedure for photocatalytic reactions

To a 10 mL reaction tube with a stir bar were added the substrate (0.4 mmol) and then 10 mg catalyst. Subsequently, 1 mL MeCN was added as the solvent. The reaction mixture was stirred for 12 h at room temperature under a 390 nm light source at 1 atm O₂ pressure (O₂ balloon). The conversion and yield were determined by GC with diphenyl as the internal standard. The conversion of the substrate and the product yield were calculated according to the following formula:

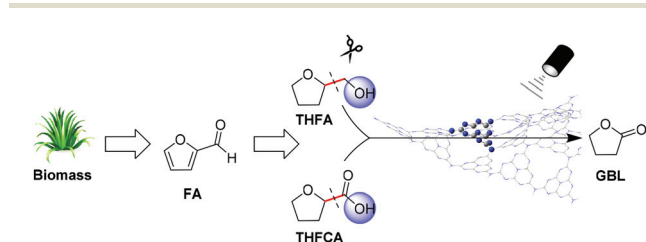
$$\text{Conversion} = (n_0 - n_1)/n_0 \times 100\%$$

$$\text{Yield} = n(\text{actual yield})/n(\text{theoretical yield}) \times 100\%$$

where n_0 is mol of the substrate before reaction and n_1 is mol of the substrate after reaction.

The apparent quantum efficiency (QE) was measured under the same photocatalytic reaction conditions. The QE was calculated according to the following formula:³¹

$$\begin{aligned} \text{QE} &= \frac{\text{Number of reacted electrons}}{\text{Number of incident electrons}} \times 100\% \\ &= \frac{\text{Number of target products}}{\text{Number of incident electrons}} \times 100\% \end{aligned}$$



Scheme 1 The strategy for the photocatalytic oxidation of furfural derivatives to prepare GBL.

General information for DFT calculations

The Gaussian 16 package³² was used for all DFT calculations. The B3LYP functional^{33,34} and 6-31G*³⁵ basis set were employed for geometry optimization of the catalyst, reactants, intermediates, and products. Vibrational frequencies were then calculated at the same level used to obtain zero-point energy (ZPE) corrections. For each transition state, only one imaginary frequency was found, whereas no imaginary frequencies were found for all the reactants, intermediates, and products. Afterward, intrinsic reaction coordinate (IRC) analysis was conducted.

Results and discussion

In order to test the photocatalytic reaction of THFA, various heterogeneous semiconductor materials were used as the catalysts initially. The results of various catalysts under identical reaction conditions are presented in Table 1. When there was no catalyst in the reaction system, THFA was not converted (entry 1). When typical semiconductors were used as the photocatalysts, such as TiO₂, WO₃, MoS₂, CdS and so on (as presented in Table 1, entries 2–7), they exhibited low reactivity for this reaction. When CNM (carbon nitride, prepared from melamine) was used as the catalyst, it exhibited relatively high catalytic activity, with 50% conversion and 44% yield. When CNU (carbon nitride, prepared from urea) was used as the catalyst, 57% conversion and 51% yield could be obtained. When M-CNU (mesoporous graphitic carbon nitride) was used as the catalyst, 72% conversion and 64% yield could be obtained. Based on the above experimental results, we speculated that the conversion from THFA to GBL was mainly dependent on the oxidizing power of the valence band and the absorbance of the semiconductor materials. According to a previous report,³⁶

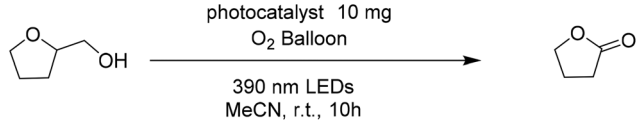
carbon nitride has a larger redox window range than most semiconductors. Furthermore, the used light source could also match the band gap of carbon nitride (entries 8–10) and the UV-Vis absorption spectra (as shown in Fig. S2†) of various semiconductor materials were able to prove this point. In addition, it seemed that different precursors may also affect the activity of carbon nitride. Better conversion and yield were obtained for reactions performed with the catalyst of M-CNU, possibly due to its higher specific surface area with much more active sites. Therefore, we separately characterized the physicochemical properties of different carbon nitrides to verify the above conjecture. As presented in Table 2, the specific surface areas of CNM, CNU and M-CNU were 18.3, 55.4 and 215.1 m² g^{−1}, respectively, according to the N₂ physical adsorption results, verifying the above conjecture. The larger specific surface area of M-CNU was mainly attributed to the mesoporous structure (Fig. 1) of the catalyst. In addition, the UV-Vis absorption of the catalysts was further investigated. As shown in Fig. 2a, CNM, CNU and M-CNU all had good absorbance at wavelengths ranging from 300 to 400 nm. The band gaps of CNM, CNU, and M-CNU were calculated to be 2.6, 2.7, and 2.6 eV, respectively, according to the Kubelka–Munk plot.³⁷ Thus, the light absorptions of these three carbon nitrides were all excellent, and this result demonstrated that

Table 2 N₂ physical adsorption results of CNM, CNU and M-CNU

Entry	Sample	<i>S</i> _{BET} ^a (m ² g ^{−1})	<i>V</i> _{pore} (cm ³ g ^{−1})	<i>d</i> _{pore} ^b (nm)
1	CNM	18.3	0.15	3.4
2	CNU	55.4	0.32	3.8
3	M-CNU	215.1	0.81	8.7

^a Multipoint BET surface area. ^b Cumulative volume of pores and average pore width determined by the BJH method.

Table 1 The photocatalytic oxidation of THFA to GBL with different catalysts^a

<div style="text-align: center;">  </div>						
Entry	Catalyst	Solvent	<i>t</i> [h]	Light sources	Conversion	Yield ^c
1	—	CH ₃ CN	10	390 nm	Trace	N.D.
2	Fe ₂ O ₃	CH ₃ CN	10	390 nm	<5%	<5%
3	Al ₂ O ₃	CH ₃ CN	10	390 nm	<5%	Trace
4	TiO ₂	CH ₃ CN	10	390 nm	34%	31%
5	WO ₃	CH ₃ CN	10	390 nm	7%	5%
6	MoS ₂	CH ₃ CN	10	390 nm	<5%	<5%
7	CdS	CH ₃ CN	10	390 nm	20%	12%
8	CNM	CH ₃ CN	10	390 nm	50%	44%
9	CNU	CH ₃ CN	10	390 nm	57%	51%
10	M-CNU	CH ₃ CN	10	390 nm	72%	64%
11 ^b	M-CNU	Neat	10	390 nm	—	0.21 mmol

^a Reaction conditions: 0.4 mmol THFA, 10 mg catalyst, 1 mL MeCN, 390 nm LED, O₂ balloon, room temperature, and 10 h. ^b Reaction conditions: 1 mL THFA, 10 mg catalyst, 390 nm LED, O₂ balloon, room temperature, and 10 h. ^c Yields were determined by gas chromatography (GC) analysis using biphenyl as the internal standard.

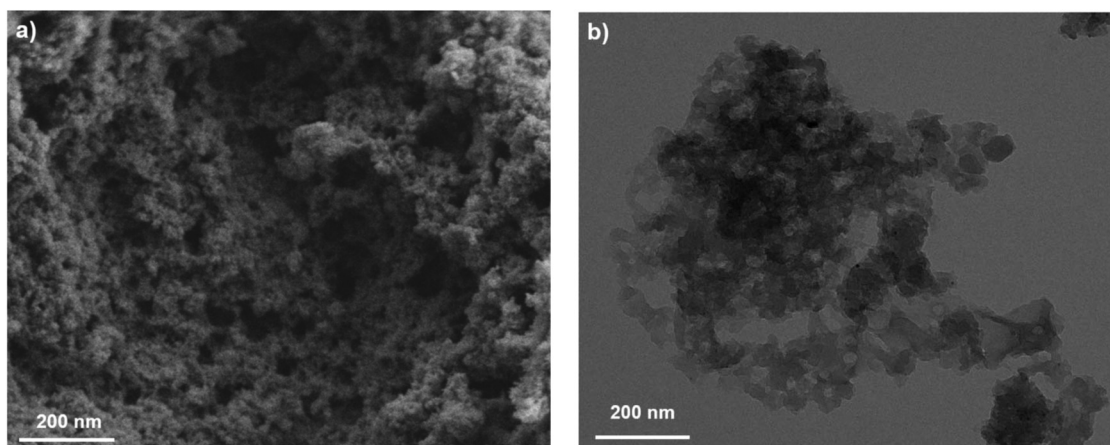


Fig. 1 SEM (a) and TEM (b) images of the M-CNU catalyst.

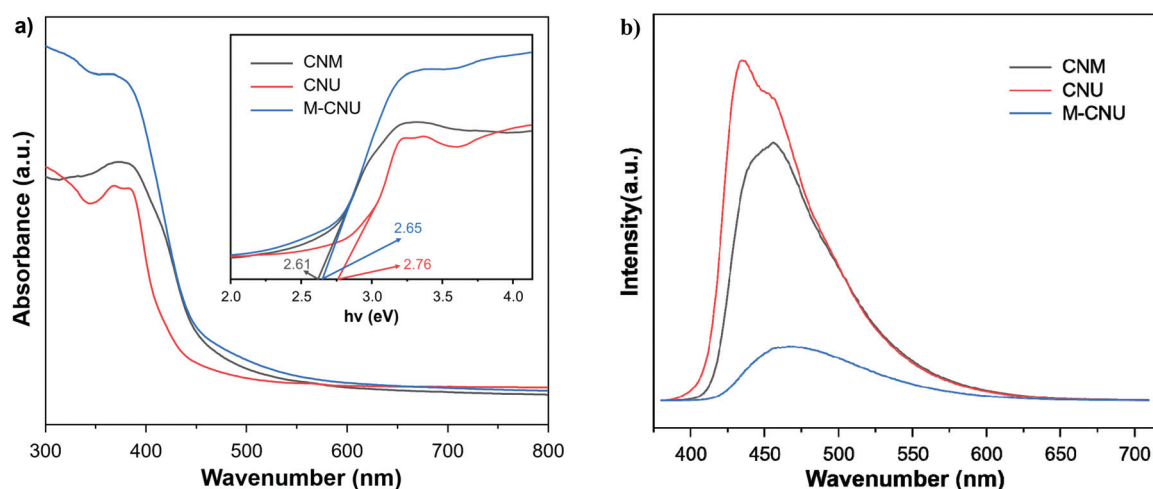


Fig. 2 UV-Vis patterns (a) and photoluminescence spectra (b) of CNM, CNU and M-CNU. Inset in (a) shows a digital photograph and the plot of the transformed Kubelka–Munk function versus the photoenergy for CNM, CNU and M-CNU samples.

the UV-Vis absorption of these three catalysts contributed little to the catalytic reactivity differences.

We also characterized the XRD patterns of the as-prepared carbon nitrides. As shown in Fig. S7,[†] two typical diffraction peaks around 12.9° and 27.7° corresponded to the intralayer long-range order and the interlayer periodic stacking which was controlled by van der Waals forces, respectively.³⁸ According to a previous report, the weak peak of the intralayer long-range order indicated that CNU and M-CNU had less intralayer hydrogen bonds, showing superior photoactivity because of the fast charge transfer between interlayers.³⁹ Besides, the relatively weak and broadened peaks at 27.7° of CNU and M-CNU indicated that the polymerization of urea gave the carbon nitride structure with less layers. Moreover, photoluminescence spectra of these three carbon nitrides were also investigated. As shown in Fig. 2b, M-CNU has the lowest electron-hole recombination rate according to the low photoluminescence intensity compared with CNM and CNU.

Therefore, low photoluminescence intensity was another factor affecting the catalytic performance on the transformation of THFA into GBL. In addition, we also tried to use solvent-free reaction conditions, and about 0.21 mmol (corresponding to a generation efficiency of $2.1 \text{ mmol g}_{\text{cat}}^{-1} \text{ h}^{-1}$) GBL could be obtained under the same reaction conditions. The effect of the reaction time on the photocatalytic oxidative cleavage of THFA to prepare GBL was investigated under the optimal reaction conditions. The mole amount of GBL at different times within 50 hours was determined respectively. The corresponding production efficiency of GBL was also calculated. As shown in Fig. 3, there was almost a linear relationship between the mole amount of GBL and the reaction time. It was worth mentioning that the production efficiency of GBL was stable, about $2.2 \text{ mmol g}_{\text{cat}}^{-1} \text{ h}^{-1}$. Based on the above experimental results, we could draw the conclusion that carbon nitride was relatively stable under these reaction conditions and could still have good reactivity after working for 50 hours. In addition, the

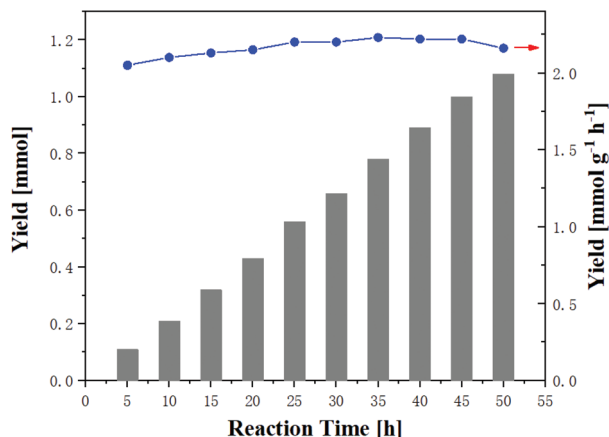
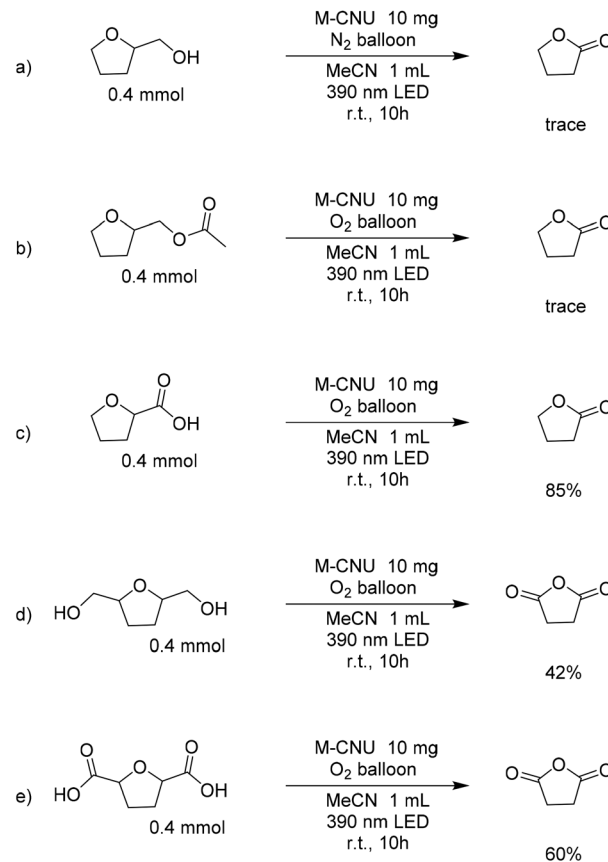


Fig. 3 The effect of the reaction time on the photocatalytic oxidation of THFA to GBL. Reaction conditions: 1 mL THFA, 10 mg catalyst, 390 nm LED, O₂ balloon, and room temperature. Yields were determined by gas chromatography (GC) analysis using biphenyl as the internal standard.

recyclability test of this catalyst was performed for five consecutive runs and the detailed experimental process is shown in the ESI.† As shown in Fig. S3,† the product yield was slightly reduced and this was mainly caused by the loss of the catalyst during the catalyst transfer process. The catalyst loss was about 3–6 wt% after each recovery. In addition, we performed XRD, XPS and SEM of the fresh catalyst (M-CNU) and the recovered catalyst respectively. The XRD (Fig. S4†) and SEM (Fig. S5†) results both confirmed the stability of the catalyst morphology. The XPS results (Fig. S6†) showed that the chemical valence states of C and N did not change significantly. In summary, the stable product yields observed herein and the characterization results of the catalyst indicated that the catalysts could be recycled and reused several times.

Validation experiments were performed under optimal reaction conditions (as shown in Scheme 2) to investigate the reaction mechanism. As a comparison, nitrogen was used as the protective gas for the reaction (entry a). Low conversion and trace GBL could be detected in this reaction system. On the basis of the above result, it could be concluded that oxygen was essential to the preparation of GBL from the photocatalytic oxidative cleavage of THFA. Additionally, in order to clarify that the H atom on the hydroxyl group was activated by the catalyst resulting in the C–C cleavage, tetrahydrofurfuryl acetate was used as the substrate (entry b). The trace target product was obtained through the analysis of the reaction solution, indicating that the activation of the hydroxyl group was crucial for this reaction. Another interesting finding was that the H atom of the carboxyl group could also be activated in the same catalytic system, and about 85% of GBL was obtained resulting from the decarboxylation oxidation. It seemed that the C–C bond of THFCA was more prone to cleavage than that of THFA. In addition, tetrahydrofurandimethanol and tetrahydrofurandicarboxylic acid, as furanyl derivatives, could also be cleaved by photocatalytic aerobic oxidation



Scheme 2 Validation experiments and other substrates.

under the same reaction conditions. The corresponding target product was succinic anhydride with the byproduct of succinic acid.

In addition, to identify the roles of different oxidative species in the photocatalytic oxidation of THFA to GBL, a series of experiments were carried out with different sacrificial agents, such as tryptophan for ¹O₂, *p*-phthalic acid for [•]OH, KI for h⁺ and *p*-benzoquinone for [•]O₂^{•−}.⁴⁰ As compared to the experiment without a sacrificial agent, the yield of GBL decreased obviously when KI or *p*-benzoquinone was used as the sacrificial agent and the yield of GBL varied little when tryptophan or *p*-phthalic acid was used as the sacrificial agent. Additionally, electron paramagnetic resonance (EPR) experiments were performed to confirm the active species of oxygen (Fig. 4). O₂^{•−} was confirmed using 5,5-dimethyl-1-pyrroline *N*-oxide (DMPO) as the spin trapper. No EPR signal was detected without light irradiation, consistent with the above experimental result (Table 3, entry 7). In addition, the possible reactions for the active oxygen species using carbon nitrides are given as follows (Scheme 3).

When incident light irradiates the surface of carbon nitrides, electrons in the valence band of the photocatalyst will be excited to transition to the conduction band, and the corresponding holes will be left in the valence band of the photocatalyst.⁴¹ Photogenerated electrons and holes are effective

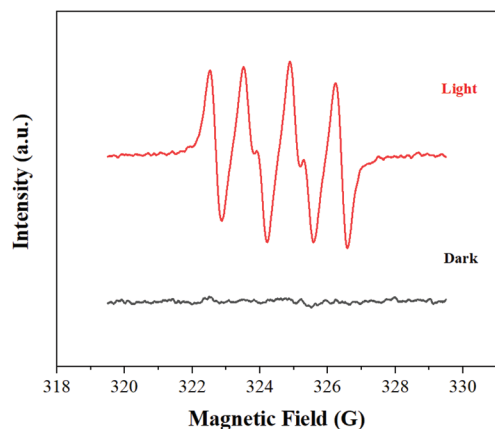
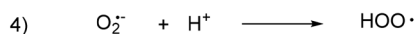
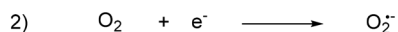
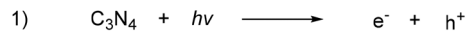


Fig. 4 Detection of the superoxide radical ($\text{O}_2^{\bullet-}$) formed by irradiated M-CNU using the spin-trap method.

Table 3 The photocatalytic oxidation of THFA to GBL with different light sources

Entry	Catalyst	Time [h]	Light source	Yield [mmol]	Yield [$\text{mmol g}^{-1} \text{h}^{-1}$]	AQE [%]
1	M-CNU	10	467 nm	0.14	1.4	0.9
2	M-CNU	10	456 nm	0.2	2.0	0.8
3	M-CNU	10	440 nm	0.23	2.3	0.9
4	M-CNU	10	427 nm	0.28	2.8	1.3
5	M-CNU	10	390 nm	0.21	2.1	2.7
6	M-CNU	10	370 nm	0.08	0.8	1.9
7	M-CNU	10	Dark	Trace	—	—

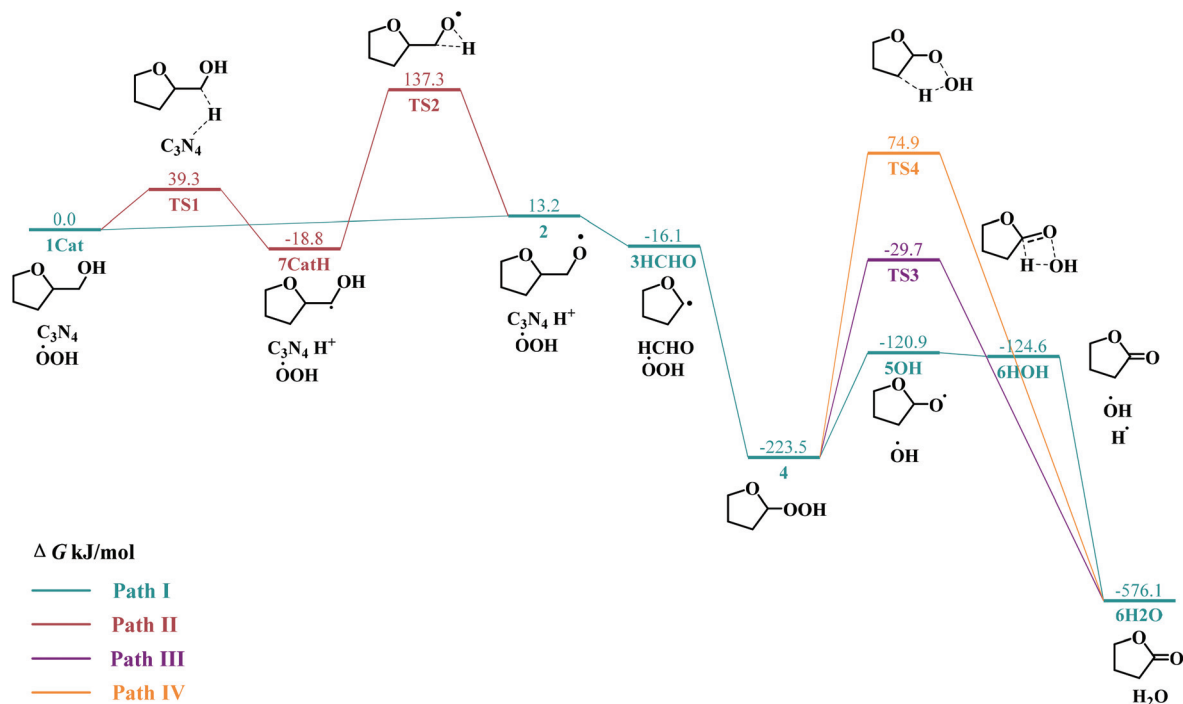
Reaction conditions: Substrate 1 mL, neat, O_2 balloon, catalyst 10 mg, and room temperature. The result was obtained by GC with biphenyl as the internal standard.



Scheme 3 The possible mechanism of active oxygen species.

tively separated. At this time, oxygen is reduced by the excited electrons from the conduction band to generate a superoxide radical anion ($\text{O}_2^{\bullet-}$),⁴² and THFA could be transformed into H^+ and alkoxy radicals in the valence band. The superoxide radical anion could be combined with H^+ to generate HOO^\bullet .

The results obtained from the above experiments indicated that this catalytic strategy afforded an efficient protocol for the transformation of THFA into GBL. Some mechanisms, involving the C–C bond cleavage of cyclic alcohols or vicinal diols *via* proton-coupled electron-transfer activation of alcohol O–H bonds,⁴³ were even proposed. To further shed light on the reaction mechanism, extensive density functional theory (DFT) calculations were performed (as shown in Scheme 4) subsequently. Initially, we ruled out direct excitation pathways due to the observation that there was no spectral overlap between the emission of the 390 nm LEDs and the absorption of THFA. The excitation of THFA might have two possibilities in this carbon nitride catalyzed photosystem. One was the direct activation of the hydroxyl group through abstracting a hydrogen by carbon nitride, yielding an alkoxy radical intermediate 2



Scheme 4 Energy profiles for the proposed reaction mechanism.

(Path I). The other one was the loss of Chydroxyl-H through a transition state TS1, with the carbon radical 7 generated. After an intramolecular hydrogen transfer reaction *via* TS2, THFA can also be transformed into the alkoxy radical intermediate 2 (Path II). The alkoxy radical makes the adjacent C–C bond unstable, which then breaks spontaneously to form the carbon radical 3 and a molecule of HCHO. Later, the product from oxygen activation ($\cdot\text{OOH}$) by carbon nitride can combine with 3, forming a stable compound 4, which transformed into the final product GBL after losing a molecule of water. Three pathways for the dehydration of 4 might occur. In Path I, as the O–O bond in 4 is unstable, it might be cleaved directly to form a hydroxyl radical and the oxygen radical intermediate 5. Then radical 5 would further lose a hydrogen to form GBL. Also, intermediate 4 might be converted into GBL in one step *via* different intramolecular dehydration reactions (Paths III and IV). From the energy profile, Path I was the most favorable pathway due to its lowest activation energy.

Conclusions

In summary, we have developed a heterogeneous metal-free photocatalytic strategy to achieve the preparation of GBL with biomass-based furfural derivatives under ambient conditions. Mesoporous graphitic carbon nitride is used as the photocatalyst and O_2 is used as the oxidant without any other additives under visible-light irradiation. Efficient preparation of GBL could be achieved with this catalytic strategy under neat reaction conditions. In addition, serious control experiments and DFT calculations were adopted to illustrate the possible reaction mechanism. The generation of the alkoxy radical intermediate is essential for the cleavage of the C–C bond, and the superoxide radical anion has been proven to be the reactive oxygen species for this reaction. In this manuscript, we expanded the photocatalytic conversion path of biomass resources and first realized the photocatalytic synthesis of GBL from biomass-based furfural derivatives.

Conflicts of interest

The authors declare no conflicts of interest.

Acknowledgements

This work was supported by the National Natural Science Foundation of China (21572212, 51821006, and 51961135104), the National Key R&D Program of China (2018YFB1501604), the Major Science and Technology Projects of Anhui Province (18030701157), the Users with Excellence Program of Hefei Science Center CAS (Grant 2019HSC-UE017), the Strategic Priority Research Program of the CAS (XDA21060101). The authors thank Hefei Leaf Biotech Co., Ltd and Anhui Kemi Machinery Technology Co., Ltd for free samples and equipment that benefited their ability to conduct this study.

Notes and references

- (a) J. Tollefson, Reality check for fossil-fuel divestment, *Nature*, 2015, **521**, 16–17; (b) N. Fabian, Economics: support low-carbon investment, *Nature*, 2015, **519**, 27–29; (c) J. Tollefson, Can the world kick its fossil-fuel addiction fast enough?, *Nature*, 2018, **556**, 422–425; (d) Q. Di, Y. Wang, A. Zanobetti, Y. Wang, P. Koutrakis, C. Choirat, F. Dominici and J. D. Schwartz, Air Pollution and Mortality in the Medicare Population, *N. Engl. J. Med.*, 2017, **376**, 2513–2522.
- T. László, E. C. Mika and Á. Németh, *Chem. Rev.*, 2018, **118**, 505–613.
- (a) R.-J. van Putten, J. C. van der Waal, E. de Jong, C. B. Rasrendra, H. J. Heeres and J. G. de Vries, *Chem. Rev.*, 2013, **113**(3), 1499–1597; (b) I. Delidovich, P. J. C. Hausoul, L. Deng, R. Pfützenreuter, M. Rose and R. Palkovits, *Chem. Rev.*, 2016, **116**(3), 1540–1599.
- S. G. Wettstein, D. M. Alonso, Y. Chong and J. A. Dumesic, *Energy Environ. Sci.*, 2012, **5**, 8199–8203.
- E. Nikolla, Y. Román-Leshkov, M. Moliner and M. E. Davis, *ACS Catal.*, 2011, **1**(4), 408–410.
- X. Li, P. Jia and T. Wang, *ACS Catal.*, 2016, **6**(11), 7621–7640; R. Mariscal, P. Maireles-Torres, M. Ojeda, I. Sádaba and M. L. Granados, *Energy Environ. Sci.*, 2016, **9**, 1144–1189.
- M. Hara, K. Nakajima and K. Kamata, *Sci. Technol. Adv. Mater.*, 2015, **16**, 034903.
- X. Li, X. Lan and T. Wang, *Green Chem.*, 2016, **18**, 638–642.
- (a) M. Hong and E. Y.-X. Chen, *Nat. Chem.*, 2016, **8**, 42–49; (b) Y. Shen, J. Zhang, N. Zhao, F. Liu and Z. Li, *Polym. Chem.*, 2018, **9**, 2936–2941.
- (a) L. Corbel-Demilly, B. Ly, D. Minh, B. Tapin, C. Especel, F. Epron, A. Cabiach, E. Guillon, M. Besson and C. Pinel, *ChemSusChem*, 2013, **6**, 2388–2395; (b) K. H. Kang, U. G. Hong, Y. Bang, J. H. Choi, J. K. Kim, J. K. Lee, S. J. Han and I. K. Song, *Appl. Catal., A*, 2015, **490**, 153–162; (c) T. J. Korstanje, J. I. van der Vlugt, C. J. Elsevier and B. de Bruin, *Science*, 2015, **350**, 298–302; (d) Y. Takeda, M. Tamura, Y. Nakagawa, K. Okumura and K. Tomishige, *Catal. Sci. Technol.*, 2016, **6**, 5668–5683; (e) K. H. Kang, S. J. Han, J. Won-Lee, T. H. Kim and I. K. Song, *Appl. Catal., A*, 2016, **524**, 206–213; (f) M. A. Hamdana, S. Loidanta, M. Jahjahb, C. Pinela and N. Perret, *Appl. Catal., A*, 2019, **571**, 71–81.
- (a) M. C. Bagley, Z. Lin, D. J. Phillips and A. E. Graham, *Tetrahedron Lett.*, 2009, **50**, 6823–6825; (b) T. M. Hansen, G. J. Florence, P. Lugo-Mas, J. Chen, J. N. Abrams and C. J. Forsyth, *Tetrahedron Lett.*, 2003, **44**, 57–59.
- (a) H. Shimizu, S. Onitsuka, H. Egami and T. Katsuki, *J. Am. Chem. Soc.*, 2005, **127**, 5396–5413; (b) T. Mitsudome, A. Noujima, T. Mizugaki, K. Jitsukawa and K. Kaneda, *Green Chem.*, 2009, **11**, 793–797; (c) K. Chung, S. M. Banik, A. G. De Crisci, D. M. Pearson, T. R. Blake, J. V. Olsson, A. J. Ingram, R. N. Zare and R. M. Waymouth, *J. Am. Chem. Soc.*, 2013, **135**, 7593–7602; (d) T. R. Blake and

- R. M. Waymouth, *J. Am. Chem. Soc.*, 2014, **136**, 9252–9255; (e) A. Díaz-Rodríguez, I. Lavandera, S. Kanbak-Aksu, R. A. Sheldon, V. Gotor and V. Gotor-Fernández, *Adv. Synth. Catal.*, 2012, **354**, 3405–3408.
- 13 X. Xie and S. S. Stahl, *J. Am. Chem. Soc.*, 2015, **137**, 3767–3770.
- 14 C. Zhu, Q. Li, L. Pu, Z. Tan, K. Guo, H. Ying and P. Ouyang, *ACS Catal.*, 2016, **6**, 4989–4994.
- 15 (a) T. Mitsudome, A. Noujim, T. Mizugaki, K. Jitsukawaa and K. Kaneda, *Green Chem.*, 2009, **11**, 793–797; (b) S. Musa, I. Shaposhnikov, S. Cohen and D. Gelman, *Angew. Chem., Int. Ed.*, 2011, **50**, 3533–3537; (c) P. Könst, S. Kara, S. Kochius, D. Holtmann, I. W. C. E. Arends, R. Ludwig and F. Hollmann, *ChemCatChem*, 2013, **5**, 3027–3032; (d) X. Li, Y. Cui, X. Yang, W. Dai and K. Fan, *Appl. Catal., A*, 2013, **458**, 63–70; (e) Y. Ryabenkova, P. J. Miedziak, D. W. Knight, S. H. Taylor and G. J. Hutchings, *Tetrahedron*, 2014, **70**, 6055–6058; (f) S. Chakraborty, P. O. Lagaditis, M. Förster, E. A. Bielinski, N. Hazari, M. C. Holthausen, W. D. Jones and S. Schneider, *ACS Catal.*, 2014, **4**, 3994–4003; (g) K. Paudel, B. Pandey, S. Xu, D. K. Taylor, D. L. Tyler, C. L. Torres, S. Gallagher, L. Kong and K. Ding, *Org. Lett.*, 2018, **20**, 4478–4481.
- 16 (a) S. A. Regenhart, C. I. Meyer, T. F. Garetto and A. J. Marchi, *Appl. Catal., A*, 2012, **449**, 81–87; (b) R. Li, J. Zhao, D. Han and X. Li, *Chin. Chem. Lett.*, 2017, **28**, 1330–1335.
- 17 M. T. Pérez-Prior, J. A. Manso, M. P. García-Santos, E. Calle and J. Casado, *J. Org. Chem.*, 2005, **70**, 420–426.
- 18 M. E. González-Núñez, R. Mello, A. Olmos and G. Asensio, *J. Org. Chem.*, 2005, **70**, 10879–10882.
- 19 C. Xiao, Z. Du, S. Li, Y. Zhao and C. Liang, *ChemCatChem*, 2020, **12**, 3650–3655.
- 20 (a) F. Parrino, M. Bellardita, E. I. García-López, G. Marci, V. Loddò and L. Palmisano, *ACS Catal.*, 2018, **8**, 11191–11225; (b) T. Chhabra, A. Bahuguna, S. S. Dhankhar, C. M. Nagaraja and V. Krishnan, *Green Chem.*, 2019, **21**, 6012–6026; (c) S. Dhingra, T. Chhabra, V. Krishnan and C. M. Nagaraja, *ACS Appl. Energy Mater.*, 2020, **3**, 7138–7148.
- 21 (a) X. Wang, K. Maeda, A. Thomas, K. Takanabe, G. Xin, J. M. Carlsson, K. Domen and M. Antonietti, *Nat. Mater.*, 2009, **8**, 76–80; (b) Y. Wang, X. Wang and M. Antonietti, *Angew. Chem., Int. Ed.*, 2012, **51**, 68–89.
- 22 G. Liao, Y. Gong, L. Zhang, H. Gao, G. Yang and B. Fang, *Energy Environ. Sci.*, 2019, **12**, 2080–2147.
- 23 L. Luo, T. Zhang, M. Wang, R. Yun and X. Xiang, *ChemSusChem*, 2020, **13**, 5173–5184.
- 24 A. Savateev, I. Ghosh, B. König and M. Antonietti, *Angew. Chem., Int. Ed.*, 2018, **57**, 15936–15947.
- 25 Z. Wu, J. Wang, S. Wang, Y. Zhang, G. Bai, L. Ricardez-Sandoval, G. Wang and B. Zhao, *Green Chem.*, 2020, **22**, 1432–1442.
- 26 T. Asano, Y. Nakagawa, M. Tamurac and K. Tomishige, *Appl. Catal., A*, 2020, **602**, 117723.
- 27 (a) J. J. Wiesfeld, M. Kim, K. Nakajima and E. J. M. Hensen, *Green Chem.*, 2020, **22**, 1229–1238; (b) L. Wei, J. Zhang, W. Deng, S. Xie, Q. Zhang and Y. Wang, *Chem. Commun.*, 2019, **55**, 8013–8016.
- 28 M. M. C. H. van Schie, W. Zhang, F. Tieves, D. S. Choi, C. B. Park, B. O. Burek, J. Z. Bloh, I. W. C. E. Arends, C. E. Paul, M. Alcalde and F. Hollmann, *ACS Catal.*, 2019, **9**(8), 7409–7417.
- 29 L. Shi, L. Liang, F. X. Wang, M. S. Liu, K. L. Chen, K. N. Sun, N. Q. Zhang and J. M. Sun, *ACS Sustainable Chem. Eng.*, 2015, **3**, 3412–3419.
- 30 T. Buntara, S. Noel, P. H. Phua, I. Melián-Cabrera, G. de Vries and H. J. Heeres, *Angew. Chem., Int. Ed.*, 2011, **50**, 7083–7087.
- 31 J. Yu, J. Zhang and M. Jaroniec, *Green Chem.*, 2010, **12**, 1611–1614.
- 32 *Gaussian 16, Revision A.01*, Gaussian Inc., Wallingford, CT, 2016.
- 33 A. D. Becke, *Phys. Rev. A: At., Mol., Opt. Phys.*, 1988, **38**, 3098.
- 34 A. D. Becke, *J. Chem. Phys.*, 1993, **98**, 1372–1377.
- 35 R. Krishnan, J. S. Binkley, R. Seeger and J. A. Pople, *J. Chem. Phys.*, 1980, **72**, 650–654.
- 36 I. Ghosh, J. Khamrai, A. Savateev, N. Shlapakov, M. Antonietti and B. König, *Science*, 2019, **365**, 360–366.
- 37 Q. Wu, Y. M. He, H. L. Zhang, Z. Y. Feng, Y. Wu and T. H. Wu, *Mol. Catal.*, 2017, **436**, 10–18.
- 38 Y. Kang, Y. Yang, L.-C. Yin, X. Kang, L. Wang, G. Liu and H.-M. Cheng, *Adv. Mater.*, 2016, **28**, 6471–6477.
- 39 M. Shalom, S. Inal, D. Neher and M. Antonietti, *Catal. Today*, 2014, **225**, 185–190.
- 40 J. Ma, D. Jin, Y. Li, D. Xiao, G. Jiao, Q. Liu, Y. Guo, L. Xiao, X. Chen, X. Li, J. Zhou and R. Sun, *Appl. Catal., B*, 2021, **283**, 119520.
- 41 A. Kudo and Y. Miseki, *Chem. Soc. Rev.*, 2009, **38**, 253–278.
- 42 F. Su, S. C. Mathew, G. Lipner, X. Fu, M. Antonietti, S. Blechert and X. Wang, *J. Am. Chem. Soc.*, 2010, **132**, 16299–16301.
- 43 (a) A. Hu, Y. Chen, J. Guo, N. Yu, Q. An and Z. Zuo, *J. Am. Chem. Soc.*, 2018, **140**, 13580–13585; (b) E. Ota, H. Wang, N. L. Frye and R. R. Knowles, *J. Am. Chem. Soc.*, 2019, **141**, 1457–1462; (c) R. Zhu, G. Zhou, J. Teng, X. Li and Y. Fu, *ChemSusChem*, 2020, **13**, 5248–5255.